Title: in vivo short TE localized 1 H MR spectroscopy of mouse cervical spinal cord at very high magnetic field (11.75T)

Mohamed Tachrount, Guillaume Duhamel, Jérôme J Laurin, Tanguy Marqueste, André Maues de Paula, Patrick Decherchi, Patrick J Cozzone, Virginie Callot, Mohamed Tachrount

Title: *in vivo* short TE localized ^{1}H MR spectroscopy of mouse cervical spinal cord at very high magnetic field (11.75T)

Short title: Short TE localized ^{1}H MR spectroscopy of mouse cervical spinal cord at 11.75T

Authors:

Mohamed Tachrount[1], Guillaume Duhamel[1], Jérôme Laurin[2], Tanguy Marqueste[2], Andre Maues de Paula[3], Patrick Decherchi[2], Patrick J. Cozzone[1], Virginie Callot[1]

Affiliations :

[1] Centre de Résonance Magnétique Biologique et Médicale, CRMBM, UMR CNRS 6612, Faculté de Médecine, Aix-Marseille Université, Marseille, France

[2] Institut des Sciences du Mouvement, ISM,, UMR CNRS 6233, Faculté des Sciences du Sport, Aix-Marseille Université, Marseille, France

[3] Service d'Anatomie Pathologique et Neuropathologie, APHM, CHU La Timone, Marseille, France

Corresponding author:

Mohamed Tachrount, PhD. Centre de Résonance Magnétique Biologique et Médicale (CRMBM), CNRS UMR 6612, Faculté de Médecine, Université de la Méditerranée, 27 bd Jean Moulin, 13385, Marseille cedex 05, France.
Phone : +33 491 324 813
Fax : +33 491 256 539
Email : mohamed.tachrount@univmed.fr

Grant support:

ANR-09-BLAN-0295-01 (TRAUMATISM project) and CNRS

Word count:

Abstract

MR Spectroscopy (MRS) provides a non-invasive assessment of metabolic information in healthy and pathological central nervous system (CNS). Whereas MRS has been extensively applied in the brain, only few spectroscopic studies of the spinal cord (SC) have been performed so far. For mice, due to additional technical challenges, *in vivo* ^{1}H MRS of the spinal cord has never been reported before the present study.

This work presents the feasibility of short TE (TE definition?) localized ^{1}H MRS, using Point Resolved Spectroscopy (PRESS) sequence, for the examination of mouse cervical spinal cord at very high magnetic field (11.75T). Several optimizations were performed to improve the static field homogeneity and to reduce physiological motion effects as well as lipid contaminations arising from spinal cord surrounding tissues. The spectrum quality and quantification, the robustness and the reproducibility of the proposed ^{1}H MRS approach were evaluated and compared to the results obtained on the thalamus.

The mean reproducibility regarding tNAA, tCr, tCho, mI and Glu quantification was 76.5 ± 12.1 % for the spinal cord and 90.0 ± 2.4 % for the thalamus. The inter-subject mean variability of these metabolites was 15.0 ± 5 and 11.4 ± 4.4 for the spinal cord and for the thalamus, respectively. The normalized amplitudes of tNAA, tCr, tCho, and Glu were significantly lower in the spinal cord than in the thalamus ($p < 0.0001$) whereas no significant difference was found for mI.

Finally, the optimized SC ^{1}H MRS sequence was applied to investigate the feasibility of detecting SC metabolic alterations following SC injury. The sequence allows reliable measurement of metabolic variations under those pathological conditions.

Introduction

Proton Magnetic Resonance Spectroscopy (^{1}H MRS) allows for *in vivo* non-invasive assessment of cerebral biochemistry. In addition, ^{1}H MRS reveals physiological alterations that are not attainable with MRI, thus contributing to its increasing application in central nervous system (CNS) studies. Whereas almost all the ^{1}H MRS studies of CNS have been conducted in the brain (1-4), it is clear that ^{1}H MRS could also be of interest in the study of several pathologies affecting the spinal cord (SC) and revealed by MRI (e.g. multiple sclerosis (MS) and amyotrophic lateral sclerosis (ALS) (5,6), spinal cord ischemia (7), spinal tumors (8), and spinal cord injury (SCI) (9)). However, very few ^{1}H MRS SC studies have been reported so far, in humans (10-14) and in rats (15-20). This could be explained by challenging experimental difficulties caused by the small size of the SC structure, the important physiological motion and the increased magnetic field heterogeneity due to surrounding bony structures. To the best of our knowledge, this study is the first account of the use of *in vivo* ^{1}H MRS for the quantification of SC metabolites in healthy or pathological mice, although transgenic mouse models are widely used to understand pathological mechanisms and to explore therapeutic approaches.

The present work demonstrates the feasibility of an optimized short TE proton spectroscopy sequence based on the Point REsolved SpectroScopy (PRESS) sequence for the investigation of the mouse spinal cord at very high magnetic field (11.75T). The shimming strategy and the acquisition method have been adapted and optimized in order to improve the static field homogeneity, and to reduce motion effects and lipid signal contamination arising from surrounding tissues. The robustness of the optimized SC protocol was evaluated and compared to results obtained in the thalamus area. Finally, the optimized sequence was

applied to preliminarily investigate the feasibility of detecting SC metabolic alterations following a SC injury (SCI).

Materials and Methods

MRI and MRS experiments were carried out on a Bruker Avance 11.75 T/89 mm vertical wide bore imager (Bruker, Ettlingen, Germany) equipped with actively shielded gradients (maximum gradient strength of 1 T/m, maximum slew rate of 9 kT/m/sec). A birdcage coil (diameter 2 cm, homogenous length 3 cm; Micro 2.5 probe; Bruker) was used for the transmission and the reception of signals.

MR Spectroscopy

MRS acquisitions were performed using a PRESS sequence with the following parameters: TE/TR = 10/4000 ms, BW = 4960 Hz, number of samples = 512, and number of averages = 16/256 without/with water suppression. Hermitian excitation pulses (0.8 ms, BW = 6750 Hz) and Shinnar-Le Roux refocusing pulses (0.8 ms, BW = 6250 Hz) were applied for the volume of interest (VOI) selection. The voxel sizes, in the dorsal-ventral, left-right, and caudal-rostral directions, were 2.0x1.8x1.1 mm^3 (VOI_{sc}~4µl) for the spinal cord and 1.5x4.5x1.5 mm^3 ($VOI_{Thalamus}$~10µl) for the thalamus. Phase cycling (8 steps) was applied to suppress signal from unwanted coherence orders. Water suppression (WS) was achieved using the VAPOR (variable power RF pulses with optimized relaxation delays) module which was interleaved with three outer volume suppression (OVS) blocks to improve localization performance (21). VAPOR consisted of seven frequency selective Hermitian RF pulses with a bandwidth of 300 Hz (~ 0.6 ppm). Each OVS block contained six spatial selective hyperbolic secant RF pulses (2.0 ms, BW ~ 10.1 kHz). The water suppressed signal and navigator signal acquisitions were interleaved. Navigator signal, which was used as reference signal, was acquired using the same VOI selection module but with a lower excitation flip angle (α=15°).

Animal Preparation

Healthy and injured male C57BL/6 mice (weight 29-36 g) were cared for and used according to a protocol approved by our institutional Committee on Ethics in animal research, in conformity with the European convention for the protection of vertebrate animals used for experimental purposes and institutional guidelines (no. 86/609/CEE November 24, 1986).

After isoflurane induction in an anesthetic chamber, the animals were kept anesthetized at a respiratory frequency of 50-70 breaths per minute by spontaneous respiration of a mixture of air and isoflurane (1.5%; mean flow rate 255 mL/min; Univentor 400 anesthesia unit, Zejtun, Malta) delivered through a dedicated nose cone. Respiration was monitored throughout the experiment, using a pressure sensor placed under the abdomen of the mouse and connected to an MR-compatible monitoring and gating system (SA Instruments, Inc., Stony Brook, NY, USA). Physiological temperature was maintained by heating the gradient cooling system to 39°C. The animals were positioned head up on an animal bed and maintained by a teeth holder and by taping their pelvis to the cradle.

In order to illustrate the potential of MRS optimized sequence, one mouse with spinal cord injury was studied. The animal was anesthetized by an intraperitoneal injection of a mixture of 100 mg/Kg of ketamine (Panpharma Laboratories, France) and 10 mg/Kg of xylazine (Bayer HealthCare, France). After a midline longitudinal skin incision over the C1-C4 spinous processes, vertebral muscles were dissected to expose the dorsal laminae and spinal processes of C3. A partial dorsolateral laminectomy on the left side of the spinal cord was performed to expose the segment C3. Perpendicular to the rostral-caudal axis of the spine, a 2-French Fogarty catheter (Edwards Lifesciences SAS, Maurepas, France) connected to an air syringe was inserted between the C2-C3 vertebra and advanced caudally for 3 mm, so that the center of the balloon rested at the C3 epidural space of the spinal cord. The balloon was then

rapidly inflated during 5 sec (10 mm^3, 25 kPa) to induce cervical spinal cord compression. Finally, muscles and skin were sutured, then antiseptic wound cleaning was performed

MR data acquisition protocol

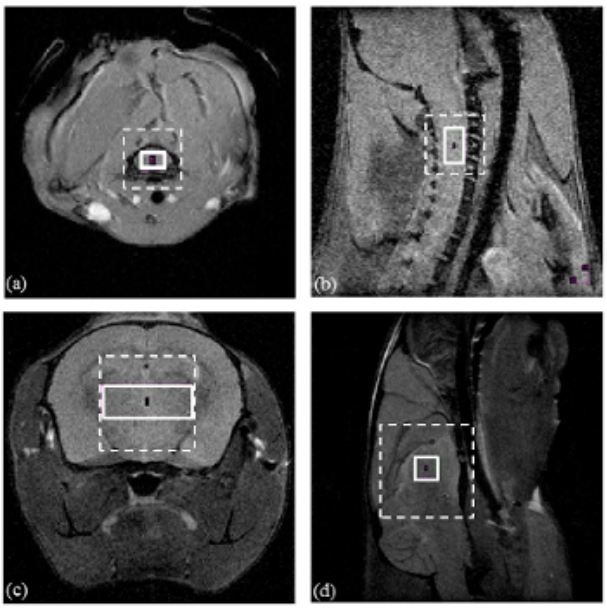

FIG. 1. Location of the selected voxels for *in vivo* ^1H MRS measurements (white rectangle) in the spinal cord (VOI_{sc}~4µl), using axial (a) and sagittal (b) T_1-weighted images, and in the thalamus ($VOI_{Thalamus}$~10µl), using axial (c) and sagittal (d) T_2-weighted images. The voxel size, in the dorsal-ventral, left-right, and caudal-rostral directions, were 2.0x1.8x1.1 mm^3 for the spinal cord and 1.5x4.5x1.5 mm^3 for the thalamus. The dashed line rectangles represent the shim voxels in the spinal cord (18 µl) and in the thalamus (22 µl).

MR data acquisitions were performed in two separate steps at the cervical spinal cord level and in the thalamus. The region of interest was aligned with the coil center and placed at the magnet isocenter in order to obtain the optimal sensitivity. Following standard spectrometer adjustments (coil tuning/matching, RF gain calibration) and fast localization imaging, the MRS VOI positioning was performed using sagittal and axial high spatial resolution T_1-weighted images for SC location (C3 level, Fig. 1a and Fig. 1b), and T_2-weighted images for thalamus location (Fig. 1c and Fig. 1d). T_1-weighted images were acquired using a FLASH sequence (22) (flip angle = 15°; TE/TR = 1.7/30.0 ms; TA = 1min 5s/3min 50s [axial/sagittal]; spatial resolution = 0.08x0.15 mm^2; slice thickness = 0.5 mm; number of slices = 6/12 [axial/sagittal]). T_2-weighted images, which provide a better delineation of the

brain structures, were acquired with a RARE sequence (23) ($TE/TE_{eff}/TR$ = 9.1/19.4/2000 ms; NA = 2; RARE Factor = 4; TA = 4min16s; number of slices = 30; slice thickness = 0.5 mm; FOV = 20x20 mm^2; Matrix = 256x256). Shimming was optimized prior the MRS acquisition, using fast localized automatic adjustment of all first- and second-order shims (FASTMAP manufacturer sequence (24)). The best shim quality, evaluated by measuring the Full Width at Half Maximum (FWHM) of a reference water spectrum, was obtained by taking shim voxels centered on the spectroscopic VOI and a volume size of about 4.2 mm^3 in the SC (i.e. including vertebra bone) and 4.7 mm^3 in the thalamus. Localized adjustments of both resonance frequency and reference gain were additionally performed to reduce the VOI location errors and to achieve the correct effective flip angle, respectively. MRS data acquisition was synchronized with breath motion to reduce artifacts arising from movement. Spectra acquisition time was about 25 minutes per location and the total protocol duration was 90 minutes.

Data processing and quantification

MRS data were processed using the jMRUI tool (version 3.0, http://www.mrui.uab.es/mrui) (25) and in-house developed software running under Matlab (The Mathworks Inc, USA). Navigator signals were applied to normalize and to correct separately each acquired water suppressed signal for eddy currents and B_0 frequency drift effects before adding them all. Following a zero filling of a factor 4, the signals acquired in SC and thalamus were multiplied by a 10-Hz and 3-Hz exponential line-broadening window function, respectively. After Fourier transform, the phases of the spectra were corrected manually and the residual water signal was subsequently removed using the HLSVD procedure (Hankel–Lanczos Singular Value Decomposition) (26) of jMRUI. Model fitting was performed in the time domain using the QUEST (quantification based on semi-parametric quantum estimation) (27) procedure of jMRUI. The metabolite basis set was quantum-mechanically simulated using GAMMA

(General Approach to Magnetic resonance Mathematical Analysis) (28) based on published chemical-shift and *J*-coupling values (29). The basis sets, simulated for the pulse sequence parameters used in this study, included 16 metabolites: alanine (Ala), aspartate (Asp), creatine (Cr), phosphocreatine (PCr), gamma-amino-butyric acid (GABA), glucose (Glc), glutamate (Glu), glutamine (Gln), glutathione (GSH), glycerophosphocholine (GPC), phosphocholine (PCho), lactate (Lac), *myo*-inositol (Ins), *N*-acetyl aspartate (NAA), *N*-acetylaspartyl glutamate (NAAG), and taurine (Tau) in accordance with the literature (27,30,31).

For SC (thalamus respectively) spectra fitting, the modeled signals chemical shift correction was limited to 25 Hz (20 Hz respectively) and the line broadening was limited to 50 Hz (40 Hz respectively). The significant macromolecular (MM) signals were estimated from initial acquired samples using QUEST. In our study, the optimal number of truncated samples was fixed to five. This number estimation was based on prior SC and thalamus metabolite nulled spectra measurements performed using an inversion recovery preparation (TR = 2.5s, TI = 700 ms) with a secant hyperbolic RF pulse of 4ms duration (data not shown) and a previous study (32).

Finally, the metabolites quantified with Cramér-Rao lower bound (estimated error of metabolite quantification) lower than 50% were included in the final neurochemical profile whereas those with lower bounds greater than 50% were classified as not detected. Metabolites with similar and strongly correlated overlapping resonances were summed (tNAA = NAA+NAAG, tCr = PCr+Cr, and tCho = PCho + GPC) and the corresponding CRBs were accordingly corrected. The Signal to Noise Ratio (SNR) was calculated using the real part of the spectrum and by dividing the NAA peak intensity by the standard deviation of the noise between 6.0 and 7.5 ppm.

Reproducibility and inter-subject variability

The reproducibility R of the quantified spectra was evaluated for both SC and thalamus, by repeating measurements at three time points on 3 mice. R was estimated for each metabolite by calculating the value of (1-SD/M)×100, where M and SD represent the normalized metabolite amplitude mean value and standard deviation obtained over the 3 measurements and the 3 mice. The inter-subject variability, V, defined by the relation V=SD/M×100, was estimated for each metabolite in the spinal cord and the thalamus using 7 and 9 healthy mice, respectively.

Spinal cord post-injury ^{1}H MRS

The preliminary investigation of metabolic alterations arising within the spinal cord following experimental injury was performed with the same protocol at days 3, 7, and 42 post-injury. The MRS VOI was located at the C3 level and included the lesion site (Fig. 4a and Fig. 4b).

Statistical analysis

All data were presented as mean ± SD. An unpaired t-test was applied for comparing spinal cord and thalamus main metabolite normalized amplitudes and results with $p<0.005$ were considered significant.

Results

Healthy mouse SC ^{1}H MRS

The averaged reference water signal FWHMs were found equal to 25.3±2.4 Hz, range 21.8 to 26.6 Hz within the spinal cord (n=7) and 22.9±3.2 Hz, range 17.0 to 26.6 Hz within the thalamus (n=9). The averaged SNR was measured to 11.9 ± 1.4 (VOI = 4 µl) for SC and 27.7 ± 4.3 (VOI = 10 µl) for thalamus. Typical ^{1}H MR spectra acquired in the SC and the thalamus of healthy mouse are presented in Fig. 2a and Fig. 2b, respectively, along with the QUEST quantification results that include estimated spectra and baseline (Fig. 2c and Fig. 2d) as well as residue (Fig. 2e and Fig. 2f).

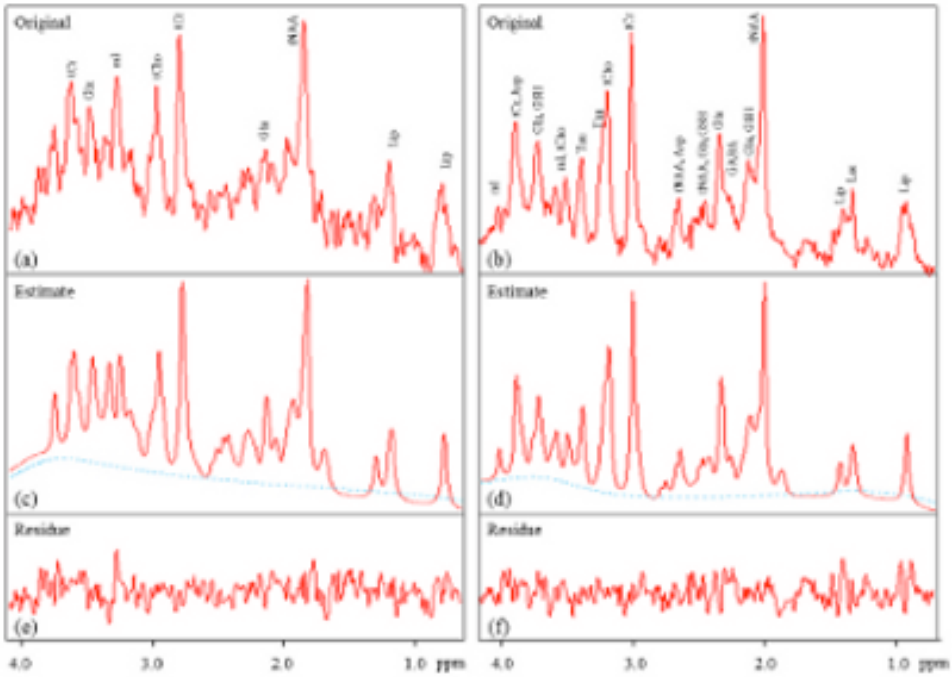

FIG. 2. (a) Typical *in vivo* healthy mouse ^{1}H spectra acquired at 11.75T from spinal cord and (b) thalamus with PRESS sequence (TR = 4s, TE = 10 ms, and NA = 256), with indication of the detected metabolite resonances. (c) Spinal cord and (d) thalamus estimated spectra and baseline (dashed line) obtained using QUEST. (e) Quantification residue corresponding to spinal cord and (f) thalamus.

The mean normalized amplitudes of detected metabolites in both SC and thalamus are presented in Fig. 3 along with their corresponding CRBs. The principal discernable metabolites in SC were tNAA, tCr, tCho, mI, and Glu (Fig. 3a). In thalamus, Ala, Asp, Gln, Tau, GABA, GSH, Glc, and Lac were additionally observed (Fig. 3b). In SC, tNAA, tCr, mI and Glu were detected with CRBs < 8% whereas tCho was quantified with CRBs < 15% (Fig. 3c). In thalamus, tNAA, tCr, tCho, mI, Glu, Tau, Gln, GABA, Ala, GSH, and Asp were quantified with CRBs < 10% whereas Glc, and Lac were quantified with CRBs < 30% (Fig. 3d). The tNAA, tCr, tCho, and Glu normalized amplitudes were significantly lower in the spinal cord than in the thalamus ($p< 0.005$). There was no significant difference between mI normalized amplitudes in the spinal cord compared to thalamus.

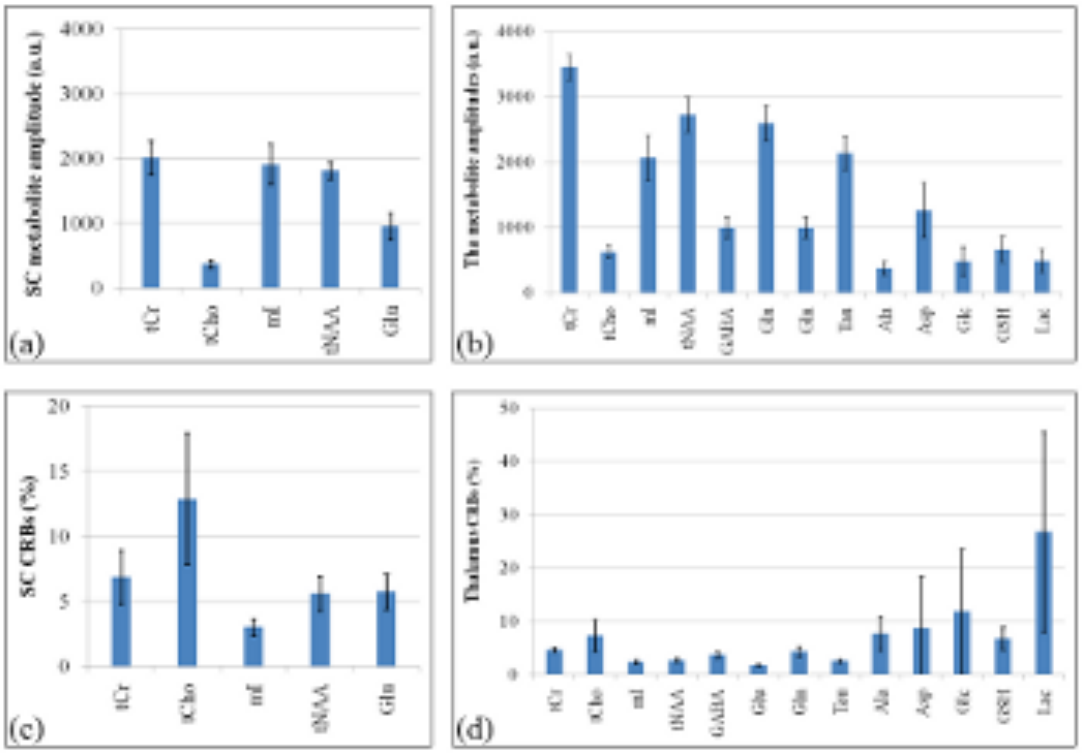

FIG. 3. Histograms of healthy mice normalized metabolite amplitude detected in SC (a) and thalamus (b) with corresponding normalized CRBs (c) and (d), respectively.

		tCr	tCho	mI	tNAA	Glu	GABA	Gln	Tau	Ala	Asp	Glc	GSH	Lac
R (%, n = 3 mice)	SC	86.4±7.0	79.7±13.3	73.0±13.3	86.2±3.3	57.2±30.0	nd	nd	nd	nd	nd	nd	nd	nd
	Tha	92.3±8.5	88.0±10.9	86.8±14.9	91.2±7.8	71.2±2.1	91.4±24.9	83.8±8.4	86.0±18.8	76.9±11.3	35.2±24.4	58.8±36.4	80.9±17.8	70.7±17.1
V (%)	SC	13.1	17.4	16.3	7.4	20.6	nd	nd	nd	nd	nd	nd	nd	nd
	Tha	5.6	15.3	16.3	9.6	10.2	16.1	16.0	11.7	28.6	33.0	45.7	29.6	36.0

Table 1. Healthy mice ^{1}H MR spectra quantification reproducibility (R) and inter-subject variability (V) in the spinal cord (SC) and the thalamus (Tha). (nd: not detected)

Spinal cord spectra quantification reproducibility (R) and inter-subject variability (V) are presented in Table 1 for each of the detected metabolites. The mean reproducibility regarding tNAA, tCr, tCho, mI and Glu quantification was 76.5 ± 12.1 % for the spinal cord and 90.0 ± 2.4 % for the thalamus. The averaged inter-subject variabilities of these metabolites within the spinal cord and thalamus were 15.0 ± 5.0 % and 11.4 ± 4.4 %, respectively. When averaging

the 13 detected metabolites for the thalamus, the mean reproducibility and inter-subject variability were equal to 78.0 ± 16.2 % and 21.0 ± 12.2 %, respectively.

Injured mouse ^{1}H MRS

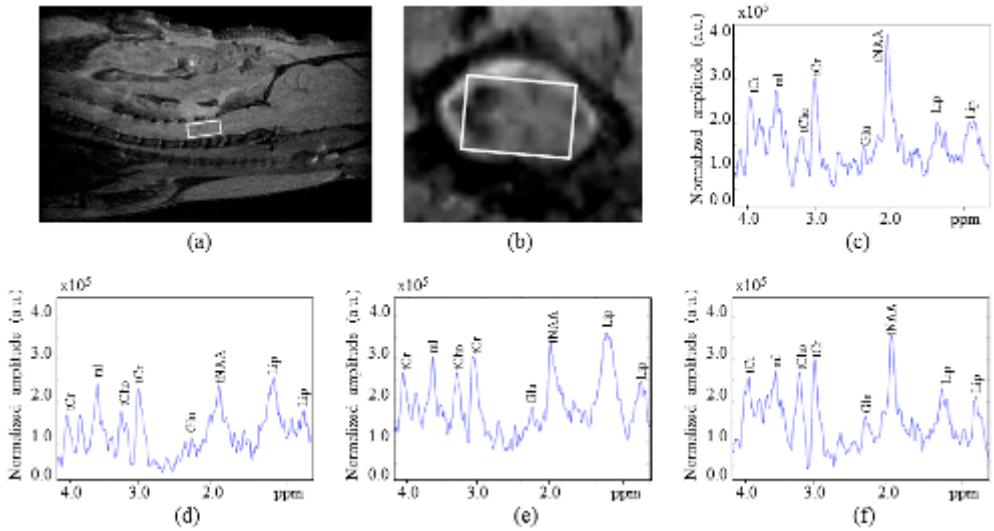

FIG. 4. Location of the selected voxel for *in vivo* ^{1}H MR spectroscopy of injured spinal cord in sagittal T_1-weighted images (a) and axial T_2^*-weighted images (b). The VOI included the lateralized lesion (b). Acquired spectra before injury (c) and 3 (d), 7 (e), and 42 (f) days post-injury. Lipid signal amplitude was observed to be more pronounced in the injured mouse than in the healthy controls, with maximum amplitude at 7 days post-injury.

The ^{1}H MRS VOI was located at the C3 level and included the lesion epicenter, as depicted on Fig. 4a and 4b. ^{1}H MR spectra acquired at 3, 7, and 42 days post-injury (dpi) are shown in Fig. 4d-f, along with a reference spectrum (Fig. 4c). The difference within the metabolites amplitude highlighted (i) the metabolic alterations and changes that occurred between healthy and injured SC, and (ii) occurring within the post-injury days. Quantitative analyses of these variations are presented on Fig. 5.

During the first week post-injury, decreases of about 50%, 15%, 8%, 13% and 49% in the tNAA, tCr, tCho, mI and Glu amplitudes were noticed compared to averaged healthy control measurements. Following the first seven days post-injury, a progressive recovery of these metabolites was observed with time. At day 42 post-injury, mI amplitude returned to the control value whereas the tNAA and the Glu presented an incomplete recovery (-15% and -

18%, respectively). In contrast, the tCr and tCho presented higher amplitudes than the control value (+15% and +13%, respectively). The variations of the tNAA, tCr, mI and Glu amplitudes were higher than the healthy mice averaged inter-subject variability whereas the tCho amplitude variations were lower.

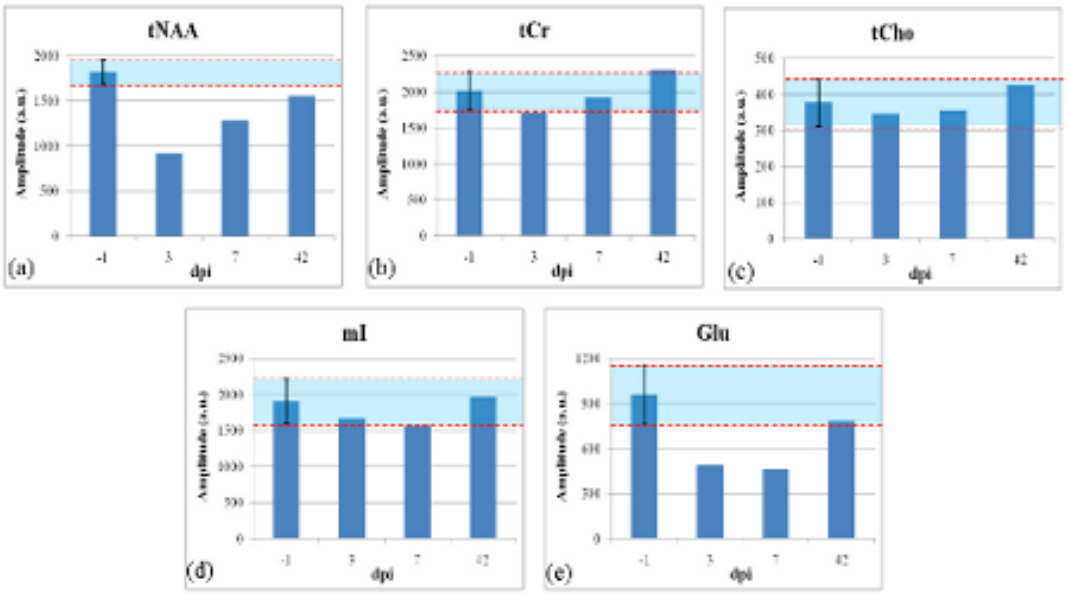

FIG. 5. SC normalized metabolite amplitudes obtained in one injured mouse at 3, 7 and 42 dpi. The mean values at -1 day post-injury (i.e before injury) correspond to the averaged healthy mice measurements (n=7) and the error bars to the mean variability.

Discussion

^{1}H MRS acquisition of the mouse spinal cord

This study reports the successful acquisition of ^{1}H MR spectra of the mouse SC despite various challenges including low sensitivity, susceptibility effects and physiological motion.

To overcome the low sensitivity inherent to the small size of the cord, several studies, performed on rats, have used implanted or surface RF coils to increase the SNR (15,16,18,19,33). Although the implanted RF coil strategy would optimize the sensitivity, this approach necessitates a particular know-how and its invasiveness may preclude early MRI/MRS measurements due to possible hemorrhage following implantation. Then, the use

of an implanted coil is not worthy for cervical SC applications. At this level, the cord is largely surrounded by skeletal muscles. In this work, SNR limitations were partially overcome by the use of a very high magnetic field strength system (11.75T) and a small volume coil well adapted to the SC morphology, allowing good quality SC and thalamus spectra acquisition with reasonable SNR value and within an acquisition time of 25 minutes.

Then, despite the large susceptibility differences between vertebral bodies, intervertebral discs, and the surrounding tissues expected at high magnetic field, the automatic shimming adjustments performed in the mouse SC allowed to obtain a shim quality (FWHM = 0.05 ppm) similar to that reported at lower field strength in rats or humans (16,18,33). The combination of the PRESS sequence with a series of OVS RF pulses interleaved with VAPOR RF pulses minimized both contamination by signals arising from outside the VOI and residual water signal. The spatially selective RF pulses transmit frequency used in our study was centered between lipids and water resonance frequencies in order to reduce the chemical shift displacement errors (CSDE), which may cause MRS VOI mislocation, complicated J-modulation patterns (34), and lipid contamination arising from surrounding tissues. The CSDE corresponding to our PRESS excitation and refocusing RF pulses were about of 14% and 15%, respectively. These displacement errors effects on acquired spectra were further reduced by using large bandwidth factor OVS RF pulses (CSDE ≈ 9%).

As physiological motion of the mouse spinal cord at the cervical level is dominated by respiration, the MRS data acquisitions were synchronized to the breathing cycle. The preparation (WS and OVS) and the VOI selection modules as well as the signal sampling were synchronized with the respiratory quiescent period to reduce these motion artifacts. To minimize the longitudinal relaxation effects that may arise when the respiratory cycle varies, relatively long repetition times, compared to metabolite longitudinal relaxation times at 11.75T (35), were additionally used. Furthermore, navigator signals acquisitions were

interleaved with water suppressed signals sampling in order to be used as reference signals. Since the double signal excitation during a single repetition time saturates the available signal and reduces the sensitivity, navigator signals were excited using a low flip angle (α=15°) and acquired after the metabolite signals acquisition. The estimated water signal loss due to the navigator acquisition was about 5%.

Mouse SC ^{1}H MRS quantification

There are only sparse reports of *in vivo* SC ^{1}H MRS quantification. The absolute metabolite concentration quantification has been reported in the case of human studies which mainly concerned cervical spinal cord, and the results presented an important variability among different groups (10-13). In other studies, relative amplitudes to unsuppressed water signal (18) or to total creatine (33) have been reported. In this study, we have used a navigator signal to normalize the metabolite amplitudes. Five metabolites were quantified within healthy mouse spinal cord with the advantage of glutamate quantification compared to studies on rats (15,16,18-20,33). The increased spectral resolution obtained at higher magnetic field might explain these results.

Given that ^{1}H MRS of the mouse spinal cord had never been performed before, thalamus spectra were acquired with the same protocol for quality comparison. Thalamus ^{1}H MRS provided thirteen metabolites which could be quantified with results in agreement with reported rodent brain studies at very high magnetic field (36,37). Although thalamus and spinal cord are likely to present different neurochemical profiles, the comparison was primarily performed to characterize the robustness and sensitivity of the optimized ^{1}H MRS PRESS sequence for mouse spinal cord studies. Then, MRS studies at the thalamus level are also of particular interest in the case of SC injury since metabolic changes are expected (38)

and since the thalamus plays an important role in the transmission of pain and in the sensori-motor pathways involved in the locomotor activity.

The robustness and the sensitivity of the technique to experimental measurement fluctuations (VOI positioning, physiological motion) and quantification errors were estimated by calculating the averaged reproducibility which was found in the order of 77 % and lower than for the same metabolites within the thalamus (90%). The inter-subject variability, which bears individual differences but also experimental measurement fluctuations, was slightly lower in the thalamus (11%) than in the spinal cord (15%) mainly due to reduced motion effects. The inter-subject variability observed in the SC was comparable or better than the values reported in human studies on healthy (11,12) or multiple sclerosis control subjects (10,13). The estimated reproducibility and inter-subject variability allow confident measurements and longitudinal follow-ups. When looking at the individual metabolites, tCho, mI, and Glu quantified amplitude presented lower reproducibility and higher variability than NAA or tCr. These quantification result variations could be attributed to baseline distortions due to residual eddy current effects and/or residual water signal as well as the macromolecular signals estimation. These signals were estimated based on a semi-parametric approach using the initial part of the acquired signal (27). The acquisition of metabolite-nulled spectra (containing only contributions from macromolecules and lipid) would provide higher precision (30). However the technique drastically increases the total acquisition time, which precludes its use in routine.

Finally, although our primary purpose in this study was not to characterize SC pathologies, the method has been applied to a preliminary model of mouse spinal cord injury. The observed initial decreases in metabolites normalized amplitudes could be attributed to axonal and neuronal damage as well as to cell population decrease due to primary cell disintegration and secondary perturbations. The progressive increases that followed could correspond to

progressive axonal recovery as well as glial activation and proliferation. Variations greater than the inter-individual variability and reproducibility have been observed, demonstrating that our optimized protocol is a potential tool to study pathological mouse SC metabolism. Although a strict comparison with reported studies is complicated by the use of different models of injury and reference signals (Cr or unsuppressed water), the results obtained in this first study are in general agreement with reported SC and brain injury studies (18,39). Further studies that are beyond the scope of this feasibility demonstration study would be required.

Conclusion

In this study, the feasibility of an optimized short TE ^{1}H MRS sequence for the mouse spinal cord investigation at very high magnetic field (11.75T) has been demonstrated. The protocol described for both acquisition and quantification allowed reliable SC metabolite amplitudes collection at the cervical level with good reproducibility and limited inter-subject variability. To the best of our knowledge, ^{1}H MRS of the mouse spinal cord has never been reported so far. This work demonstrates that the challenges of mouse SC 1H MRS can be overcome. It may therefore open new perspectives to study various pathological conditions provided by transgenic mouse models and deepen the understanding of the diseases by providing quantitative information complementary to MRI.

Acknowledgments

This work received the support of the CNRS (Centre National de la Recherche Scientifique, UMR 6612), and ANR (Agence Nationale de la Recherche, ANR-09-BLAN-0295-01). We thank Yann Le Fur and Hélène Ratiney for advice with spectra processing and quantification.

Figure legends

Tables

References

1. Soares DP, Law M. Magnetic resonance spectroscopy of the brain: review of metabolites and clinical applications. Clin Radiol 2009;64(1):12-21.
2. van der Graaf M. In vivo magnetic resonance spectroscopy: basic methodology and clinical applications. Eur Biophys J;39(4):527-540.
3. Marino S, Ciurleo R, Bramanti P, Federico A, Stefano ND. 1H-MR spectroscopy in traumatic brain injury. Neurocrit Care;14(1):127-133.
4. Morita N, Harada M, Otsuka H, Melhem ER, Nishitani H. Clinical Application of MR Spectroscopy and Imaging of Brain Tumor. Magn Reson Med Sci 2010;9(4):167-175.
5. Losseff NA, Webb SL, O'Riordan JI, Page R, Wang L, Barker GJ, Tofts PS, McDonald WI, Miller DH, Thompson AJ. Spinal cord atrophy and disability in multiple sclerosis. A new reproducible and sensitive MRI method with potential to monitor disease progression. Brain 1996;119 (Pt 3):701-708.
6. Thorpe JW, Kidd D, Moseley IF, Thompson AJ, MacManus DG, Compston DA, McDonald WI, Miller DH. Spinal MRI in patients with suspected multiple sclerosis and negative brain MRI. Brain 1996;119 (Pt 3):709-714.
7. Kumral E, Polat F, Güllüoglu H, Uzunköprü C, Tuncel R, Alpaydin S. Spinal ischaemic stroke: clinical and radiological findings and short-term outcome. Eur J Neurol 2011;18(2):232-239.
8. Sahgal A, Bilsky M, Chang EL, Ma L, Yamada Y, Rhines LD, Létourneau D, Foote M, Yu E, Larson DA, Fehlings MG. Stereotactic body radiotherapy for spinal metastases: current status, with a focus on its application in the postoperative patient. J Neurosurg Spine 2011;14(2):151-166.

9. Cadotte DW, Fehlings MG. Spinal cord injury: a systematic review of current treatment options. Clin Orthop Relat Res 2011;469(3):732-741.

10. Blamire AM, Cader S, Lee M, Palace J, Matthews PM. Axonal damage in the spinal cord of multiple sclerosis patients detected by magnetic resonance spectroscopy. Magn Reson Med 2007;58(5):880-885.

11. Cooke FJ, Blamire AM, Manners DN, Styles P, Rajagopalan B. Quantitative proton magnetic resonance spectroscopy of the cervical spinal cord. Magn Reson Med 2004;51(6):1122-1128.

12. Edden RAE, Bonekamp D, Smith MA, Dubey P, Barker PB. Proton MR spectroscopic imaging of the medulla and cervical spinal cord. J Magn Reson Imaging 2007;26(4):1101-1105.

13. Gomez-Anson B, MacManus DG, Parker GJ, Davie CA, Barker GJ, Moseley IF, McDonald WI, Miller DH. In vivo 1H-magnetic resonance spectroscopy of the spinal cord in humans. Neuroradiology 2000;42(7):515-517.

14. Henning A, Schär M, Kollias SS, Boesiger P, Dydak U. Quantitative magnetic resonance spectroscopy in the entire human cervical spinal cord and beyond at 3T. Magn Reson Med 2008;59(6):1250-1258.

15. Balla DZ, Faber C. In vivo intermolecular zero-quantum coherence MR spectroscopy in the rat spinal cord at 17.6 T: a feasibility study. MAGMA 2007;20(4):183-191.

16. Bilgen M, Elshafiey I, Narayana PA. In vivo magnetic resonance microscopy of rat spinal cord at 7 T using implantable RF coils. Magn Reson Med 2001;46(6):1250-1253.

17. Erschbamer M, Oberg J, Westman E, Sitnikov R, Olson L, Spenger C. 1H-MRS in spinal cord injury: acute and chronic metabolite alterations in rat brain and lumbar spinal cord. Eur J Neurosci 2011;33(4):678-688.

18. Qian J, Herrera JJ, Narayana PA. Neuronal and axonal degeneration in experimental spinal cord injury: in vivo proton magnetic resonance spectroscopy and histology. J Neurotrauma 2010;27(3):599-610.

19. Silver X, Ni WX, Mercer EV, Beck BL, Bossart EL, Inglis B, Mareci TH. In vivo 1H magnetic resonance imaging and spectroscopy of the rat spinal cord using an inductively-coupled chronically implanted RF coil. Magn Reson Med 2001;46(6):1216-1222.

20. Zelaya FO, Chalk JB, Mullins P, Brereton IM, Doddrell DM. Localized 1H NMR spectroscopy of rat spinal cord in vivo. Magn Reson Med 1996;35(4):443-448.

21. Tkác I, Starcuk Z, Choi IY, Gruetter R. In vivo 1H NMR spectroscopy of rat brain at 1 ms echo time. Magn Reson Med 1999;41(4):649-656.

22. Haase A, Frahm J, Matthaei D, Hanicke W, Merboldt KD. FLASH imaging. Rapid NMR imaging using low flip-angle pulses. J Magn Res 1986;67:258-266.

23. Hennig J, Nauerth A, Friedburg H. RARE imaging: a fast imaging method for clinical MR. Magn Reson Med 1986;3(6):823-833.

24. Gruetter R. Automatic, localized in vivo adjustment of all first- and second-order shim coils. Magn Reson Med 1993;29(6):804-811.

25. Naressi A, Couturier C, Devos JM, Janssen M, Mangeat C, de Beer R, Graveron-Demilly D. Java-based graphical user interface for the MRUI quantitation package. MAGMA 2001;12(2-3):141-152.

26. Pijnappel WWF, vanDenBoogaart A, deBeer R, van Ormondt D. SVD-based quantification of magnetic resonance signals. J Magn Res 1992;97:122-134.

27. Ratiney H, Sdika M, Coenradie Y, Cavassila S, van Ormondt D, Graveron-Demilly D. Time-domain semi-parametric estimation based on a metabolite basis set. NMR Biomed 2005;18(1):1-13.

28. Smith SA, O.Levante T, Meier BH, Ernst RR. Computer Simulations in Magnetic Resonance. An Object-Oriented Programming Approach. J Magn Res 1994;106 (1):75-105.

29. Govindaraju V, Young K, Maudsley AA. Proton NMR chemical shifts and coupling constants for brain metabolites. NMR Biomed 2000;13(3):129-153.

30. Gottschalk M, Lamalle L, Segebarth C. Short-TE localised (1)H MRS of the human brain at 3 T: quantification of the metabolite signals using two approaches to account for macromolecular signal contributions. NMR Biomed 2007.

31. Posse S, Otazo R, Caprihan A, Bustillo J, Chen H, Henry P-G, Marjanska M, Gasparovic C, Zuo C, Magnotta V, Mueller B, Mullins P, Renshaw P, Ugurbil K, Lim KO, Alger JR. Proton echo-planar spectroscopic imaging of J-coupled resonances in human brain at 3 and 4 Tesla. Magn Reson Med 2007;58(2):236-244.

32. Ratiney H, LeFur Y, Sdika M, Cavassila S. Short Echo Time H1 Chemical Shift Imaging data quantification in the mouse brain at 11.7T using a constrained parametric macromolecular model. Proceedings of Joint Annual ISMRM-ESMRM Meeting 2010; Stockholm, Sweden.

33. Erschbamer M, Oberg J, Westman E, Sitnikov R, Olson L, Spenger C. (1) H-MRS in spinal cord injury: acute and chronic metabolite alterations in rat brain and lumbar spinal cord. Eur J Neurosci 2011.

34. Edden RAE, Schär M, Hillis AE, Barker PB. Optimized detection of lactate at high fields using inner volume saturation. Magn Reson Med 2006;56(4):912-917.

35. de Graaf RA, Brown PB, McIntyre S, Nixon TW, Behar KL, Rothman DL. High magnetic field water and metabolite proton T1 and T2 relaxation in rat brain in vivo. Magn Reson Med 2006;56(2):386-394.

36. Lei H, Poitry-Yamate C, Preitner F, Thorens B, Gruetter R. Neurochemical profile of the mouse hypothalamus using in vivo 1H MRS at 14.1T. NMR Biomed 2010;23(6):578-583.

37. Mlynárik V, Cudalbu C, Xin L, Gruetter R. 1H NMR spectroscopy of rat brain in vivo at 14.1Tesla: improvements in quantification of the neurochemical profile. J Magn Reson 2008;194(2):163-168.

38. Likavcanova K, Urdzikova L, Hajek M, Sykova E. Metabolic changes in the thalamus after spinal cord injury followed by proton MR spectroscopy. Magn Reson Med 2008;59(3):499-506.

39. Schuhmann MU, Stiller D, Skardelly M, Bernarding J, Klinge PM, Samii A, Samii M, Brinker T. Metabolic changes in the vicinity of brain contusions: a proton magnetic resonance spectroscopy and histology study. J Neurotrauma 2003;20(8):725-743.